CONSOLIDATION OF RANDOMLY HETEROGENEOUS CLAY STRATA

Eduardo E. Alonso, Escuela Técnica Superior de Ingenieros de Caminos, Canales y Puertos, Universidad Politécnica de Barcelona, Spain; and Raymond J. Krizek, Technological Institute, Northwestern University

A simulation procedure is used to analyze the influence of a randomly varying coefficient of permeability on the one-dimensional consolidation settlement of clay layers. The method of analysis involves (a) simulating of soil profile when the basic characteristics of the homogeneous random function describing the soil permeability are known, (b) making the governing field equation discrete by means of an implicit finite difference scheme, and (c) statistically analyzing the resulting sample population when the simulation has been performed a sufficient number of times. When compared with results determined by the classical deterministic approach, the application of this analysis to a specific case shows significant differences and allows the use of standard procedures in significance testing, rather than the single estimate provided by the deterministic case, to make decisions at a given significance level.

THE classical theory of consolidation incorporates two constitutive relations in its derivation: Darcy's law, which governs the flow of water through the pores of the soil, and Hooke's law, which governs the deformational behavior of the soil skeleton. In the one-dimensional situation, each of these relations involves one material parameter, the coefficient of permeability k_x in the case of flow and the coefficient of volume change m_x in the case of deformation; both are usually assumed to be constant. However, Alonso and Krizek (1) have shown that the parameters defining the soil behavior vary randomly in space and are conveniently described by a random function of spatial coordinates. In this paper the process of one-dimensional consolidation of randomly heterogeneous strata subjected to a constant load is studied. Only the effect of a random variation will be considered because the effect of deterministic heterogeneity has been studied elsewhere (5). An approach of this kind will enable us to (a) conveniently describe the complexity of the heterogeneous variation in soil properties; (b) formulate the problem by considering, in an unambiguous way, the random variation of the soil; and (c) provide probabilistic answers that indicate a range of possible values with an associated confidence level, rather than a single deterministic estimate. This will be demonstrated by studying the dissipation of pore-water pressures and the increase in the degree of consolidation for a consolidating clay layer.

CONSOLIDATION EQUATION

Generally, k_x and m_x are both functions of position and the effective vertical stress within the consolidating layer. However, under the hypothesis of small strains, little error is obtained by considering k_x and m_x as functions of only the spatial coordinates. Therefore, the increment of volume change undergone by an element of soil can be explained solely in terms of the time-dependent changes in the void ratio e, and the

Publication of this paper sponsored by Committee on Mechanics of Earth Masses and Layered Systems.

continuity equation for the flow of pore water can be written as

$$\frac{\partial}{\partial x}\left[\frac{k_x(x)}{\gamma_w}\frac{\partial u_e}{\partial x}\right] = \frac{\partial e}{\partial t} \tag{1}$$

where u_e denotes the excess of pore-water pressure, and γ_w is the unit weight of water. Considering the definition of m_x, equation 1 becomes

$$\frac{1}{\gamma_w}\frac{\partial u}{\partial x}\left[k_x(x)\frac{\partial u}{\partial x}\right] = -m_x(x)\frac{\partial \bar{\sigma}}{\partial t} \tag{2}$$

where $\bar{\sigma}$ represents the effective vertical stress, which can be readily expressed in terms of the total applied stress σ, and u_e as $\bar{\sigma} = \sigma - u_e$. If time-dependent variations of the externally applied load are not considered, equation 2 may be expressed as

$$\frac{1}{\gamma_w}\frac{\partial}{\partial x}\left[k_x(x)\frac{\partial u_e}{\partial x}\right] = m_x(x)\frac{\partial u_e}{\partial t} \tag{3}$$

which, in terms of the coefficient of consolidation, $c_x(x) = k_x(x)/m_x(x)\gamma_w$, becomes

$$\frac{\partial^2 u_e}{\partial x^2} + \frac{1}{k_x(x)}\frac{dk_x(x)}{dx}\frac{\partial u_e}{\partial x} = \frac{1}{c_x(x)}\frac{\partial u_e}{\partial t} \tag{4}$$

If $k_x(x)$ and $c_x(x)$ are assumed to be random functions $K(x)$ and $C(x)$ of the space coordinate x, the differential equations given above become random differential equations for the excess pore pressure. Such equations are analytically untractable mainly because of the nonlinearity in the random component of the equation, and the only suitable approach currently seems to be the use of a simulation procedure in conjunction with some numerical technique and a digital computer. Although this approach can be costly if an extensive parameter study is undertaken, the answers for the specific cases studied here are complete in that the full probability structure of the solution, including first and second moments, is a natural output of the procedure. The first step toward the solution requires a method whereby random processes can be generated from basic characteristics.

SIMULATION OF RANDOM COEFFICIENTS

If $k_x(x)$ and $m_x(x)$ are considered to be random functions, there is usually a positive correlation between them, and any simulation procedure must account for this fact if rather conservative results are to be avoided. To simulate multivariate processes, Shinozuka (6) proposed methods that depend on a knowledge of the cross-spectra function between the two processes. This situation presents a major difficulty in this problem because no data are available to find such a cross-spectra function between the coefficient of permeability and the coefficient of compressibility. Two continuous or quasi-continuous records of soil permeability and compressibility would be required in the same location, provided both processes can be shown to be homogeneous in the stochastic sense.

However, when the type of soil does not change much with depth, the changes in permeability can be associated with similar changes in the coefficient of volume change

(5). In such cases, c_x in equation 4 can be considered constant. As a matter of fact, the condition of homogeneity of records (in the stochastic sense) is not really satisfied if rather different types of soil are included in the same record, and the homogeneity condition must be invoked to enable the randomness of soils to be analyzed in some detail. This also implies that there is no significant change of soil type within the layer undergoing consolidation, and little error is introduced by considering c_x as a constant instead of as a random function. Therefore, equation 4 reduces to

$$\frac{\partial^2 u_e}{\partial x^2} + \frac{1}{K(x)} \frac{dK(x)}{dx} \frac{\partial u_e}{\partial x} = \frac{1}{c_x} \frac{\partial u_e}{\partial t} \tag{5}$$

where c_x is now a constant and independent of position. When the following changes are made in the variables,

$$X = x/H \tag{6}$$

$$T = \frac{c_x t}{H^2} \tag{7}$$

$$u = \frac{u_e}{u_0} = \frac{u_e}{\sigma_0} \tag{8}$$

where H is half of the thickness of the layer, and u_0 is the initial constant increment of pore pressure (equal to the total applied stress σ_0), equation 5 becomes

$$\frac{\partial^2 u}{\partial X^2} + \frac{1}{K^*(X)} \frac{dK^*(X)}{dX} \frac{\partial u}{\partial X} = \frac{\partial u}{\partial T} \tag{9}$$

where $K^*(X) = K(XH)$. Equation 9 can be more conveniently expressed as

$$\frac{\partial^2 u}{\partial X^2} + \frac{d}{dX} [\ell n\ K^*(X)] \frac{\partial u}{\partial X} = \frac{\partial u}{\partial T} \tag{10}$$

which involves the random coefficient $\ell n\ K^*(X)$. If the properties of the random process defining the permeability in the soil are known, the main concern is now directed toward the simulation of $\ell n\ K^*(X)$.

A homogeneous normally distributed process Z(x) can be represented as (6)

$$Z(x) = \sigma_z \left(\frac{2}{N}\right)^{1/2} \sum_{k=1}^{N} \cos\ (\omega_k x - \varphi_k) \tag{11}$$

where σ_z is the standard deviation of the process, N is a large positive integer (to ensure normality), ω_k is a random variable that is distributed with a density function $S_z(\omega)/\sigma_z^2$ [where $S_z(\omega)$ is the two-sided power spectra of the process as a function of the frequency in terms of cycles per unit of spatial length ω], and φ_k is a random variable that is uniformly distributed in the interval 0 to 2π. This representation can be used for the permeability of the soil if the conditions of homogeneity and normality hold.

[Although more efficient techniques for the simulation of multidimensional processes have been proposed for the case in which the spectral distribution is not obtainable in closed form (7), the present problem, which involves a one-dimensional process with a simple power spectra function, can be adequately handled by equation 11 and requires relatively little computation.]

Since we are dealing with statistically homogeneous layers, the first condition is generally satisfied; however, there are important reasons why a normal representation of the coefficient of permeability is not realistic. For example, a negative permeability makes no sense physically, and its logarithm is undetermined mathematically; this gives rise to difficulties in the process of simulation. However, if permeability is thought to be governed by the pore-size distribution, a log-normal representation seems more appropriate: The most salient features of a log-normal distribution are its positive skewness and definition for positive values only. Physical substantiation for this concept is provided by the process of particle breakage, which leads to a log-normal distribution of particle sizes (3, 4). However, when the coefficient of variation of a log-normal distribution becomes small, it resembles a normal distribution.

Since the logarithm of a log-normal distribution is a normal distribution (referred to random variables), it is worthwhile to investigate the possibility of a representing $\ln K^*(X)$ in the form given in equation 11. Consider a two-dimensional random vector, $\overline{W} = (W_1, W_2)$, of two jointly distributed and correlated normal random variables and define the transformation

$$(Y_1, Y_2) = \overline{Y} = \overline{g}(\overline{W}) = [g_1(W_1, W_2), g_2(W_1, W_2)] \tag{12}$$

where

$$Y_1 = g_1(W_1, W_2) = \exp[W_1] \tag{13}$$

$$Y_2 = g_1(W_1, W_2) = \exp[W_2] \tag{14}$$

Since the transformation given in equations 13 and 14 is monotonic and one-to-one, the joint probability density function of Y_1 and Y_2 can be written as

$$f_{Y_1, Y_2}(y_1, y_2) = f_{W_1, W_2}[h_1(y_1, y_2), h_2(y_1, y_2)]\,|J| \tag{15}$$

where $\overline{h} = (h_1, h_2)$ denotes the inverse transformation of $\overline{g} = (g_1, g_2)$ and $|J|$ is the Jacobian of the $\overline{h}$ transformation:

$$|J| = \begin{vmatrix} \dfrac{\partial h_1}{\partial y_1} & \dfrac{\partial h_1}{\partial y_2} \\ \dfrac{\partial h_2}{\partial y_1} & \dfrac{\partial h_2}{\partial y_2} \end{vmatrix} = \frac{1}{y_1 y_2} \tag{16}$$

However, since W_1 and W_2 are jointly correlated and normally distributed, we can write

$$f_{W_1, W_2}(w_1, w_2) = \frac{1}{2\pi\sigma_1\sigma_2\sqrt{1-\rho_{12}^2}} \exp\left\{-\frac{1}{2(1-\rho_{12}^2)}\left[\left(\frac{w_1-\mu_1}{\sigma_1}\right)^2 - 2\rho_{12}\left(\frac{w_1-\mu_1}{\sigma_1}\right)\left(\frac{w_2-\mu_2}{\sigma_2}\right) + \left(\frac{w_2-\mu_2}{\sigma_2}\right)^2\right]\right\} \tag{17}$$

where ρ_{12} is the correlation coefficient between W_1 and W_2 and is defined by

$$\rho_{12} = \frac{C_{12}}{\sigma_1\sigma_2} = \frac{1}{\sigma_1\sigma_2} E[(W_1 - \mu_1)(W_2 - \mu_2)] \tag{18}$$

where C_{12} is the covariance between W_1 and W_2. Consider now that W_1 and W_2 are two specific random variables, which are defined at points x_1 and x_2 from a normal stationary random process $W(x)$. Since $W(x)$ is assumed to be stationary, the mean and variance of the process are constant along x, and the probability density function of the random vector $\overline{Y}$, given by equation 15, can be written as

$$f_{Y_1, Y_2}(y_1, y_2) = \frac{1}{y_1 y_2 2\pi\sigma^2\sqrt{1-\rho^2}} \exp\left\{-\frac{1}{2\sigma^2(1-\rho^2)}[(\ell n\, y_1 - \mu)^2 - 2\rho(\ell n\, y_1 - \mu)(\ell n\, y_2 - \mu) + (\ell n\, y_2 - \mu)^2]\right\} \tag{19}$$

where ρ, σ^2, and μ represent the correlation coefficient, variance, and mean of the process W respectively.

Assume now that the transformation $\overline{g}$ is defined in a continuous manner for the entire process $W(x)$, and thus a new process $Y(x)$ is originated by the relationship

$$W(x) = \ell n\, Y(x) \tag{20}$$

Then, the autocorrelation function of $Y(x)$, defined as the expected value of the product Y_1Y_2 of two random variables of the process $\overline{Y}(x)$ for any two points 1 and 2, becomes

$$R_Y(1, 2) = E[Y_1Y_2] = \int_0^\infty \int_0^\infty y_1 y_2 f_{Y_1, Y_2}(y_1, y_2)\, dy_1 dy_2 \tag{21}$$

Using equation 19 with equation 21, we get

$$E[Y_1Y_2] = \int_0^\infty \int_0^\infty \frac{dy_1 dy_2}{2\pi\sigma^2\sqrt{1-\rho^2}} \exp\left\{-\frac{1}{2\sigma^2(1-\rho^2)}[(\ell n\, y_1 - \mu)^2 - 2\rho(\ell n\, y_1 - \mu)(\ell n\, y_2 - \mu) + (\ell n\, y_2 - \mu)^2]\right\} \tag{22}$$

Note that, if $W(x)$ is a homogeneous process, ρ is only a function of the distance between

points 1 and 2. Calling this distance τ, using the subscript W for the parameters of the process W(x), and introducing in equation 22 the change of coordinates $v_1 = \ell n\, y_1 - \mu$ and $v_2 = \ell n\, y_2 - \mu$, we are able to write equation 22 as

$$R_Y(\tau) = \frac{\exp(2\mu_W)}{2\pi\sigma_W^2\sqrt{1-\rho_W^2}} \int_{-\infty}^{\infty} \int_{-\infty}^{\infty} \exp\left\{\frac{1}{2\sigma_W^2(1-\rho_W^2)}[v_1^2 - 2\rho_W v_1 v_2 + v_2^2]\right\}$$

$$\exp(v_1 + v_2)dv_1 dv_2 \tag{23}$$

which can be further reduced to

$$R_Y(\tau) = \beta\exp(2\mu_W) \int_{-\infty}^{\infty} \exp(-\alpha v_1^2 + v_2)dv_1$$

$$\left\{\int_{-\infty}^{\infty} \exp[-\alpha v_2^2 + v_2(2\alpha_W v_1 + 1)]dv_2\right\} \tag{24}$$

where

$$\alpha = \tfrac{1}{2}\sigma_W^2(1 - \rho_W^2) \tag{25}$$

and

$$\beta = \tfrac{1}{2}\pi\sigma_W^2\sqrt{1 - \rho_W^2} \tag{26}$$

On integration in v_2, equation 24 transforms to

$$R_Y(\tau) = \sqrt{\frac{\pi}{a}}\,\beta\exp(2\mu_W) \int_{-\infty}^{\infty} \exp\left[-\alpha(1 - \rho_W^2)v_1^2 - (-1 - \rho_W)v_1 + \frac{1}{4\alpha}\right]dv_1 \tag{27}$$

and finally transforms to

$$R_Y(\tau) = \exp[2\mu_W + \sigma_W^2(1 + \rho_W)] \tag{28}$$

In terms of the autocovariance functions $C_Y(\tau)$ and $C_W(\tau)$ of processes Y and W, equation 28 becomes

$$C_Y(\tau) + \mu_Y^2 = \exp[2\mu_W + \sigma_W^2 + C_W(\tau)] \tag{29}$$

where μ_Y designates the mean of the Y process. Note, however, that, if Y(x) has a log-normal distribution and at every point $W = \ell n\, Y$, the mean and variance of W can be expressed as

$$\mu_W = \ell n\, \mu \left(\frac{1}{\sqrt{Y}}\right)^2_W \tag{30}$$

and

$$\sigma^2_W = \ell n\, (V^2_Y + 1) \tag{31}$$

where V_Y represents the coefficient of variation of Y. If Equations 30 and 31 are introduced into equation 29, we get

$$C_W(\tau) = \ell n \left[\frac{C_Y(\tau)}{\mu^2_Y} + 1\right] \tag{32}$$

Note in all these derivations that the process Y can be identified with the soil permeability $K^*(X)$, and W with its natural logarithm. Therefore, if $K^*(X)$ is a homogeneous log normally distributed process, its logarithm is also homogeneous. Note in Equation 32 that $C_W(\tau)$ depends only on the shift τ, and it is normally distributed. This allows us to perform the simulation of $\ell n\ K^*(X)$ according to equation 11. The following successive steps are required:

1. Analyze the record of soil permeability and find its autocovariance function $C_Y(\tau)$;
2. Use equation 32 to derive $C_W(\tau)$, the autocovariance function of $\ell n\ K^*(X)$;
3. Obtain the power spectra density function of $\ell n\ K^*(X)$ by use of a numerical procedure and the Fourier transform of $C_w(\tau)$; and
4. Apply equation 11 to the process $\ell n\ K^*(X)$, whereby the standard deviation σ_z is given by equation 31 and the frequencies W_K are distributed in accordance with the unit two-sided power spectra function derived in step 3.

As shown in equation 6, the spatial coordinate X is actually dimensionless; therefore, if we denote the dimensionless frequency $\omega_k H$ by F_k, equation 11 can be written as

$$\ell n\,[K^*(X)] = \sigma_{\ell n\ K^*(X)} \left(\frac{2}{N}\right)^{1/2} \sum_{k=1}^{N} \cos(F_k X - \varphi_k) \tag{33}$$

where the frequencies F_k are distributed in accordance with the density function $S_{\ell n\ K^*}(F)/\sigma^2_{\ell n\ K^*}$ (see Appendix), where H is the characteristic length of the problem (half the thickness of the consolidating layer in this case).

METHOD OF SOLUTION

A finite difference technique has been used to solve the differential equation for each realization of the random process, $\ell n\ K^*(X)$. Since implicit schemes generally allow larger spacings in the time domain than explicit schemes without sacrificing convergence and since a simulation procedure requires a large number of computations, the reduction in computer time afforded by the implicit schemes made them more suitable for this problem. In particular, the Crank-Nicholson implicit scheme (2) has been used here because of its accuracy and simple formulation.

Figure 1a shows the domain of integration of equation 10. The time domain extends from 0 to ∞, and the spatial domain has a finite length, namely, the depth of the layer undergoing consolidation. A discrete solution at the nodal points of a rectangular mesh (defined by its finite space and time increments, h and k) was sought by means of a difference approximation for the differential operators appearing in equation 10. If we consider a central difference approximation of the derivatives at point P in Figure 1a, a good compromise for the space derivative consists of the following average values for the central difference at j and j+1:

$$\frac{\partial u}{\partial X} = \tfrac{1}{2}\left(\frac{u_{i+1,\,j+1} - u_{i-1,\,j+1}}{2h} + \frac{u_{i+1,\,j} - u_{i-1,\,j}}{2h}\right) \tag{34}$$

$$\frac{\partial^2 u}{\partial X^2} = \tfrac{1}{2}\left(\frac{u_{i+1,\,j+1} - 2u_{i,\,j+1} + u_{i-1,\,j+1}}{h^2} + \frac{u_{i+1,\,j} - 2u_{i,\,j} + u_{i-1,\,j}}{h^2}\right) \tag{35}$$

$$\frac{\partial L}{\partial X} = \tfrac{1}{2}\left(\frac{L_{i+1,\,j+1} - L_{i-1,\,j+1}}{2h} + \frac{L_{i+1,\,j} - L_{i-1,\,j}}{2h}\right) \tag{36}$$

where L stands for $\ell n\ K^*(X)$. For $\partial u/\partial T$, the central difference at point P is

$$\frac{\partial u}{\partial T} = \frac{u_{i,\,j+1} - u_{i,\,j}}{k} \tag{37}$$

Inserting these expressions into equation 10 and denoting the grid parameter k/h^2 by λ, we get

$$\begin{aligned}\frac{16}{\lambda}(u_{i,\,j+1} - u_{i,\,j}) = {} & (L_{i+1,\,j+1} - L_{i-1,\,j+1} + L_{i+1,\,j} - L_{i-1,\,j}) \\ & \cdot (u_{i+1,\,j+1} - u_{i-1,\,j+1} + u_{i+1,\,j} - u_{i-1,\,j}) \\ & + 8(u_{i+1,\,j+1} - 2u_{i,\,j+1} + u_{i-1,\,j+1} + u_{i+1,\,j} - 2u_{i,\,j} + u_{i-1,\,j})\end{aligned} \tag{38}$$

As i varies from 1 (zero depth) to M (full depth of the layer), equation 38 can be viewed as a set of linear equations for each elapsed time j, and these can be expressed as

$$[A]^j\{u\}^{j+1} = \{b\}^j \tag{39}$$

with the following convention:

$$a^j_{k,\,k-1} = L_{k+1} - L_{k-1} - 4 \qquad j = 2, 3, \ldots \tag{40}$$

$$a^j_{k,\,k} = 8(1/\lambda + 1) \qquad k = 2, 3, \ldots, M - 1 \tag{41}$$

$$a^j_{k,\,k+1} = -4 - L_{k+1} + L_{k-1} \tag{42}$$

$$\{u\}^{j+1} = [u_1^{j+1},\ u_2^{j+1} \ldots u_M^{j+1}] \quad j = 1, 2, 3, \ldots \tag{43}$$

$$b_k^j = 8/\lambda u_k^j + (L_{k+1} - L_{k-1})(u_{k+1}^j - u_{k-1}^j) + 4(u_{k+1}^j - 2u_k^j + u_{k-1}^j)$$

$$k = 2, 3, \ldots, M - 1$$

$$j = 2, 3, \ldots \tag{44}$$

The remaining coefficients in equations 40, 41, and 42 are 0, except for the boundary conditions at k=1 and K=M. For the example case of free drainage at both ends, we get

$$a_{1,1} = 1;\ a_{M,M} = 1 \tag{45}$$

and

$$b_1^j = 0;\ b_M^j = 0 \quad j = 2, 3, \ldots \tag{46}$$

Note that the system of equations given by equation 39 is nonsymmetric but is banded; in fact, equations 40, 41, and 42 show that the bandwidth is 3, which allows the required storage and computation to be reduced substantially. The procedure just described does not require a constant time increment. Rather, since the method is stable for large values of the parameter λ, the possibility exists of varying the time increment to reduce the number of steps up to a given time.

Previous known solutions of the consolidation equation with a constant coefficient of permeability or with a deterministic variation of the coefficient of permeability show a decrease in the pore pressure at any point until almost zero excess pore pressure is reached. Not only the pore pressure decreases with time, but the rate of decay also decreases. Therefore, the error in the solution is expected to vary with both the increment of time used and the total elapsed time. This provides a means for maintaining the accuracy of the results approximately constant thoughout the region of integration, provided we adapt the time-dependent function describing the inverse of the time increment to the curve describing the rate of decrease of the excessive pore pressure with time. In reality, a discrete approximation is more suitable for actual applications. Figure 1b shows four successive increments of time computed with this criterion. The curve of $1/\Delta T(T)$ versus T corresponds to the rate of decrease of the degree of consolidation; this actually represents the mean rate of decrease of the excess pore pressure in the layer. If a simplified expression is chosen for the degree of consolidation with constant soil coefficients, we have

$$U = 1 - \frac{8}{\pi^2} \exp\left(-\frac{\pi^2 T}{4}\right) \tag{47}$$

and the rate of decrease of U is proportional to $\exp(-\pi^2 T/4)$. Then, the first time increment, $1/\Delta T_1$, is identified with 1 in the curve of Figure 1b, and the remaining increments are computed according to the number of different time increments desired. Other criteria can be used to find time increments according to the time at which the solution is desired. A computer program was written to perform the simulation of the proposed problem.

Figure 2 shows a simplified flow chart of the simulation process, which includes

(a) the simulation of the ℓn K*(X) process, (b) the strategy used to fix the time increments, (c) the specification of the initial and boundary conditions, (d) the solution of the resulting system of linear equations for each elapsed time, (e) the computation of the derived parameters (mainly the degree of consolidation), and (f) the statistical analysis of the desired quantities.

ANALYSIS OF SPECIFIC CASE

The simulation process associated with the general flow chart shown in Figure 2 can be summarized as follows. First, a sample soil profile with a permeability variation is artificially generated in the computer by the techniques explained. Second, the initial excess pore pressure is allowed to dissipate through this artificially generated medium until a given degree of consolidation is reached; the significant variables of this process (mainly the excess pore pressure and the degree of consolidation) are recorded for each elapsed time. Third, the first two steps are repeated many times to get a statistically satisfactory number of realizations of the time-dependent variations in the excess pore pressure and the degree of consolidation. Finally, a statistical analysis is performed on the set of derived sample populations.

The initial selection of increments in the time domain can be done on the basis of the method previously described. However, if better computer efficiency is desired, more satisfactory time increments can always be obtained for the specific problem under consideration by using a trial process in which the initial selection of increments is used as a starting point. The selection of the spatial increment of the finite difference mesh is, however, more closely related to the probabilistic aspects of the problem. In fact, the criterion for the selection of the space increment should be an accurate representation of the random process defining the natural logarithm of the permeability coefficient. A suitable criterion is suggested by the special form of equation 33, since the oscillations of the process in the X direction are governed by the cosine modulation of this equation. In particular, if F_{max} represents the maximum frequency component of the process describing ℓn K*(X), a maximum number of $F_{max}/2\pi$ cycles per unit of length X would be obtained in a representation of the form given in equation 33. When the number of points n_p needed to numerically define a cycle is fixed, an estimate of the necessary number of layer divisions N_p for a given process with F_{max} is easily computed from

$$N_p = 2F_{max}\, n_p/2\pi \tag{48}$$

since 2 is the maximum dimensionless length in this case.

The preceding development will be demonstrated for a practical situation by analyzing the consolidation of a 66-ft-thick (20-m), randomly heterogeneous clay layer that is freely drained at both ends and the total stress distribution that is uniform with depth. The clay layer is assumed to have a randomly varying (constant mean) permeability distribution with depth, but it can be conveniently represented by a homogeneous random function whose underlying probability distribution is well described by a log-normal model.

This study involves four different values for the coefficient of variation of the permeability process V_{K^*}: 0.1, 0.325, 0.7, and 1.1 corresponding to variances of 0.01, 0.1, 0.4, and 0.8 respectively for the derived ℓn K*(X) process. These values cover the range of variation likely to be encountered in the permeability of relatively homogeneous clayey soils. These cases were approximated in an actual situation by the special form of the normalized (unit area) power spectra density function shown in Figure 3. This function was chosen arbitrarily with the following considerations in mind. Equation 32, which described the autocorrelation function of the ℓn K*(X) process, gives an indication of the frequency content of this process in terms of the behavior of the K*(X) process.

Figure 1. Finite difference approximation.

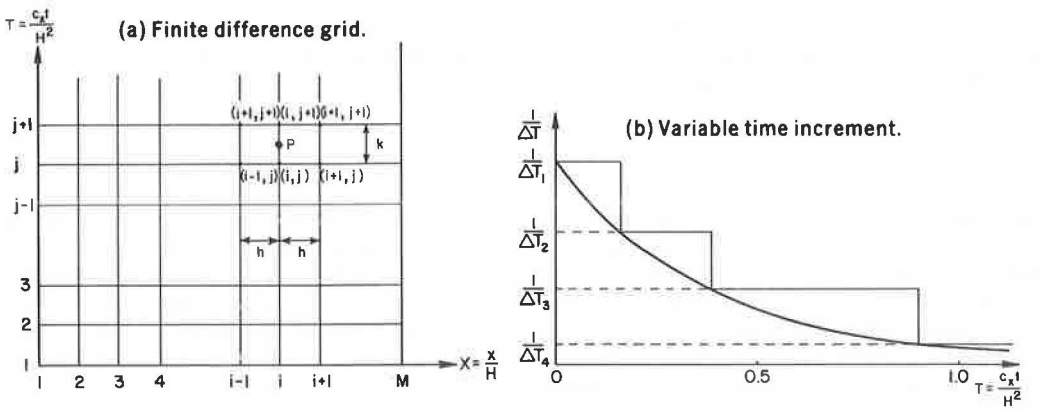

Figure 2. Simulation procedure.

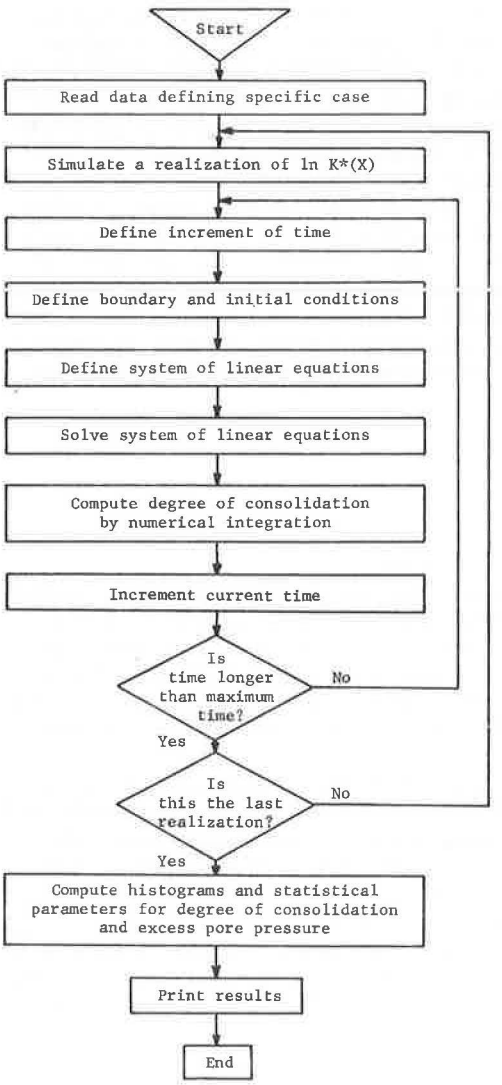

Figure 3. Power spectra function for specific case.

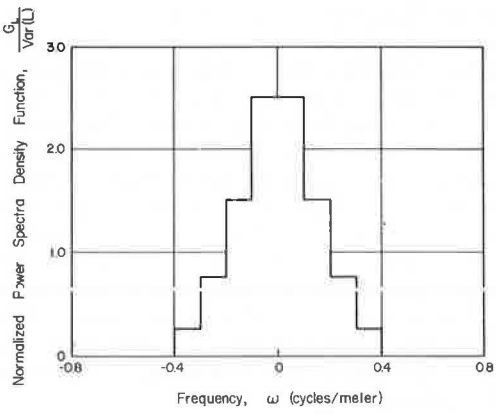

In fact, if μ_{K^*} is considered to be 1, the rate of decay of the autocorrelation function of $\ell n\, K^*(X)$ is $C'_{K^*}(\tau)/[1 + C_{K^*})\tau)]$, where C'_{K^*} is the rate of decay of the autocorrelation function of the $K^*(X)$ process.

For autocorrelation functions, $C_{K^*}(\tau)$, of the form $\exp(-\alpha\tau)$, the derived autocorrelation function of $\ell n\, K^*(X)$ will decay at a slower rate than $C_{K^*}(\tau)$, and consequently the low frequency components of the associated power spectra will be enhanced. Note, however, that this tendency is attenuated for autocorrelation function of the form $\exp(-\alpha\tau)\cos 2\pi\beta\tau$ because of the negative lobes of this representation. In any case, it does not seem that frequencies larger than the maximum ones associated with $K^*(X)$ will appear in $\ell n\, K^*(X)$. However, dominant frequency ranges between 0 and 0.5 m^{-1} were commonly encountered in the analysis of actual field records. Therefore, the hypothetical power spectra function shown in Figure 3 does not seem to differ much from real situations. These considerations have been treated in detail by Alonso and Krizek (1).

According to equation 48, 40 intervals in the definition of the finite difference mesh in the X direction give $n_p = 10\pi$ points for the definition of a cycle in the worst case; this figure was judged to be sufficiently accurate for this analysis. After a number of trials using the classical consolidation equation, the following criteria were used to determine the time increments:

1. $\Delta T = 0.025$, if $0 \leq T < 0.25$;
2. $\Delta T = 0.05$, if $0.25 \leq T < 0.6$;
3. $\Delta T = 0.1$, if $0.6 \leq T < 1.0$;
4. $\Delta T = 0.15$, if $1.0 \leq T < 1.5$; and
5. $\Delta T = 0.25$, if $T \geq 1.5$.

This distribution also satisfies the criteria given previously for the variable time increment. One hundred realizations were performed in each one of the four simulations [corresponding to the four different variances of the $\ell n\, K^*(X)$ process]. For a maximum time factor of 1, it took less than 4 min on a CDC 6400 computer to perform a complete simulation for the above-mentioned conditions.

The relevant results obtained from this simulation are shown in Figures 4 through 9. Figure 4 shows three typical realizations (out of 100 performed) of the degree of consolidation U versus the time factor T for a coefficient of variation of 1.1 for the soil permeability. Histograms of the values assumed for U at a time factor of T = 0.5 are shown in Figure 5 for the four cases studied. Note how the histogram spreads over the values of U when the coefficient of variation for $K^*(X)$ increases. Parallel to this increase in the variance of the soil permeability increases is a reduction in the mean of the degree of consolidation. This tendency is better shown in Figure 6, in which U has been plotted against T for values of $T < 1$. Curves corresponding to the mean values and one standard deviation of dispersion are shown, and the deterministic solution is given by the classical theory. Several histograms are superimposed in these figures to give an idea of the amount of dispersion.

The field equation given by equation 10 shows clearly that the mean value of the excess pore pressure does not satisfy the classical one-dimensional consolidation equation. In fact, by taking expectations of both sides of equation 10, by letting $M(X) = (d/dX)\,[\ell n\, K^*(X)]$, and by interchanging derivation and expectation operators, we get

$$\frac{\partial^2 \bar{u}}{\partial X^2} + E\left[M(X)\,\frac{\partial u}{\partial X}\right] = \frac{\partial \bar{u}}{\partial T} \tag{49}$$

Since M(X) and u(X) are obviously correlated, the second term on the left-hand side of equation 49 is not zero, and consequently it modifies the usual one-dimensional consolidation equation. However, the decrease in the mean degree of consolidation with an increase in V_{K^*} can be explained on the basis of physical grounds only. In fact, when the coefficient of variation of the soil permeability increases, there is a larger dis-

Figure 4. Realizations for degree of consolidation versus time.

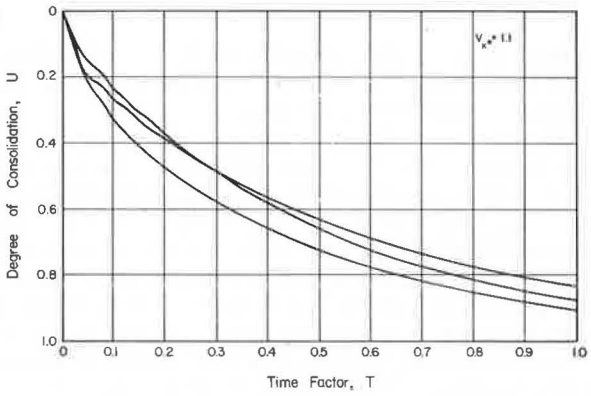

Figure 5. Degree of consolidation at T = 0.5 for four cases.

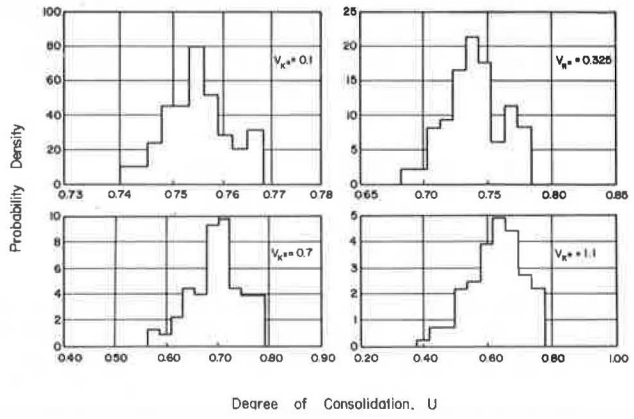

Figure 6. Degree of consolidation versus time.

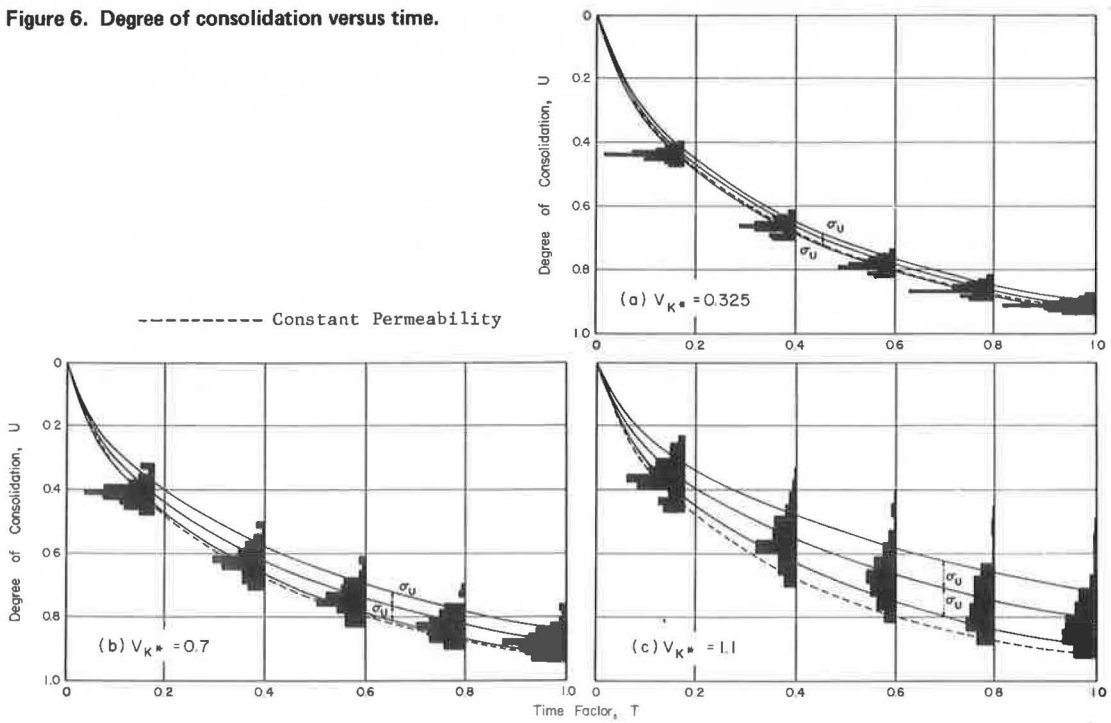

persion of the soil permeability, and this can reach very low values at some places. These low values tend to govern the entire process of consolidation, even though highly permeable regions contribute to a significantly different mean value.

Figure 7 shows the decrease in the mean value of the degree of consolidation for increasing dispersion of the permeability coefficient. If only the mean value ($\overline{U}$ curves) is considered, the curves in Figure 7 represent deviations of nearly 20 percent from the values predicted by classical consolidation theory; however, much larger deviations can be found in the dispersion observed in the histograms. The correct prediction of the degree of consolidation at a given time must be based on some confidence level, and the procedures of significance testing must be used. Figure 7 also shows the increase in the standard deviation of the degree of consolidation, σ_U, with V_{K^*} for several different time factors. The limited information provided by this example indicates that the σ_U versus V_{K^*} relationships are nearly linear in some cases. No regular pattern was observed with respect to the elapsed time.

Figure 8 shows two typical realizations (corresponding to a time factor of 0.5 and a coefficient of variation of soil permeability of 1.1) of the pore pressure developed in the consolidating layer, and these are computed with those realizations predicted by classical consolidation theory. The values of the excess pore pressure at the middepth of the layer were statistically analyzed and plotted against time in Figure 9, and histograms at several time factors are shown to illustrate the variability expected.

In the case of the degree of consolidation, increases in the standard deviation and in the mean values of the pore pressure are observed for increasing dispersion of the soil permeability. Note the skewed character of the histograms for both the degree of consolidation and the excess pore pressure, especially for high values of elapsed time. Any significance testing must take this feature into account, because the skewness of the distributions toward small values of the degree of consolidation and pore pressure increases the chances of reaching smaller degrees of consolidation when compared with the results from symmetrical distributions with the same variance.

SUMMARY AND CONCLUSIONS

A simulation technique has been used to analyze the influence of a randomly heterogeneous soil permeability on the one-dimensional consolidation of a clay layer subjected to a constant load. After the governing field equation was made discrete by an implicit Crank-Nicholson finite difference scheme, a digital computer was used to implement a step-by-step marching procedure in the time dimension. The simulation technique for the process defining the random soil variability depends on the stationary character of the soil permeability and its underlying log-normal probability distribution.

It was assumed that the changes in the coefficient of consolidation of the soil are reflected in the permeability changes; this is approximately the case if the type of soil does not change appreciably within the consolidating layer. If this is not the case, the governing field equation will contain two different correlated random processes as random coefficients, and its simulation will require an explicit knowledge of such a cross-correlation; this latter knowledge is currently difficult to obtain. The simulation procedure involves

1. Generation of a realization of the properties of the soil according to its probability structure,
2. Application of the Crank-Nicholson method to derive a step-by-step procedure that involves the solution of a system of simultaneous linear equations at each step,
3. Use of a numerical integration procedure to obtain the degree of consolidation at each elapsed time,
4. Computation of pore-pressure histograms at selected locations, and
5. Determination of the degree of consolidation with its corresponding statistical parameters (mean and variance).

Steps 4 and 5 are undertaken after the entire simulation has been completed; that is,

Figure 7. Variation of statistical parameters for degree of consolidation.

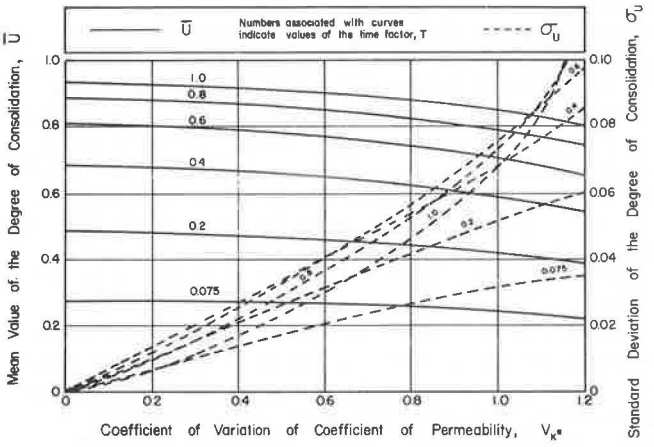

Figure 8. Realizations of pore pressure versus depth.

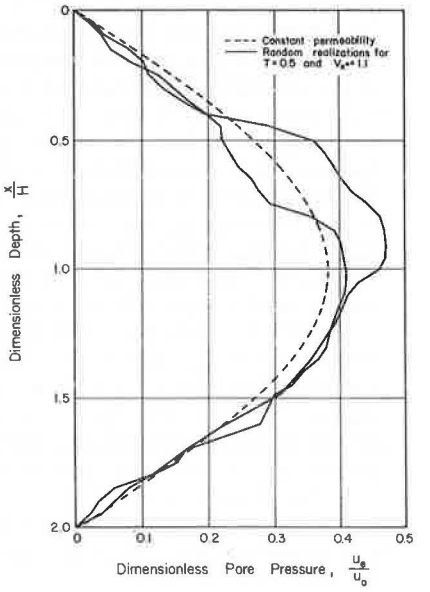

Figure 9. Pore pressure versus time.

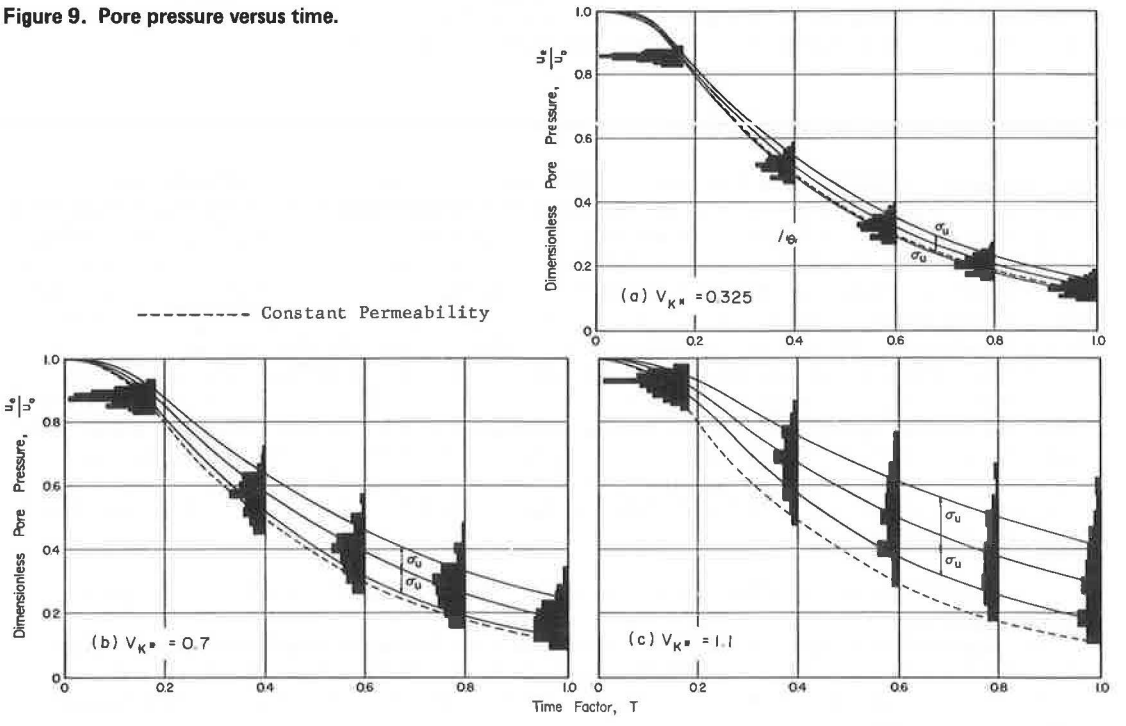

after steps 1, 2, and 3 have been performed the desired number of times. This method has been applied to a particular case, and an attempt has been made to represent as nearly as possible a real situation based on previous results. Four levels of dispersion of the coefficient of soil permeability were successively simulated to evaluate its influence; however, the same power spectra structure of the process describing soil properties was used in all the cases.

Within the limitations given, the following conclusions can be made.

1. The simulation method is a versatile tool for analyzing the influence of heterogeneous soil properties; unlike methods that rely on second-order moments, it is able to give more complete probabilistic answers but is limited in that general conclusions are costly to obtain.
2. The dispersion of soil permeability around its mean value results in a reduction in the degree of consolidation for a given time, as indicated by the mean values, which are progressively smaller than those obtained from the classical one-dimensional equation when the dispersion of the permeability coefficient increases. Therefore, if the true random coefficient of permeability (or its associated coefficient of consolidation) is replaced by its mean value, unsafe results are obtained in that a given degree of consolidation will take more time than predicted.
3. The randomness associated with the degree of consolidation introduces the possibility of obtaining results that are rather different than those predicted by the classical theory. Decisions concerning the amount of settlement expected at a given time should be based on a desired confidence level, and adequate importance must be given to the skewed character (toward smaller degrees of consolidation) of the resulting distributions.
4. Pore pressures behave qualitatively similar to their derived parameter, the degree of consolidation; thus, not only is the dispersion of the pore pressure affected by the dispersion of the coefficient of soil permeability, but also the mean is shifted to a higher value (which results in a lower value of the degree of consolidation) than that predicted by the theory of one-dimensional consolidation. The results may differ substantially from those obtained by the classical theory, and distributions skewed toward increasing values of the pore pressure are observed as time increases.

REFERENCES

1. E. E. Alonso and R. J. Krizek. Stochastic Formulation of Soil Properties. Proc., 2nd International Conference on Applications of Statistics and Probability in Soil and Structural Engineering, Aachen, Germany, 1975.
2. J. Crank and P. Nicholson. A Practical Method for Numerical Evaluation of Solutions of Partial Differential Equations of the Heat Conduction Type. Proc., Cambridge Philosophical Society, Cambridge, England, 1947, pp. 50-67.
3. B. Epstein. The Mathematical Description of Certain Breakage Mechanisms Leading to the Logarithmico-Normal Distribution. Journal of Franklin Institute, Vol. 244, 1947, pp. 471-477.
4. F. Kottler. The Distribution of Particle Sizes. Journal of Franklin Institute, Vol. 250, 1950, pp. 339-356, 419-441.
5. R. L. Schiffman and R. E. Gibson. Consolidation of Nonhomogeneous Clay Layers. Journal of Soil Mechanics and Foundations Division, American Society of Civil Engineers, Vol. 90, No. SM5, 1964, pp. 1-30.
6. M. Shinozuka. Simulation of Multivariate and Multidimensional Random Processes. Journal of Acoustical Society of America, Vol. 49, No. 1, 1971, pp. 357-367.
7. M. Shinozuka and C. M. Jan. Digital Simulation of Random Processes and Its Applications. Journal of Sound and Vibration, Vol. 25, No. 1, 1972, pp. 111-128.

APPENDIX

DISTRIBUTION OF DIMENSIONLESS FREQUENCIES

To find the probability distribution function of the dimensionless frequencies F consider first the influence of the dimensionless variable $X = x/H$ on the two-sided power spectra $S_A(\omega)$ of a homogeneous random process A(x). If $R_A(\tau)$ is the autocorrelation function, we have by definition

$$S_A(\omega) = 4\int_0^\infty R_A(\sigma)\cos 2\pi\omega\tau d\tau \tag{50}$$

If $\tau = \tau^* H$ (where τ^* is a dimensionless lag parameter) and $\omega = F/H$ (where F is a dimensionless frequency), a change of variables allows the expression for $S_A(\omega)$ to be written as

$$S_A(\omega) = 4H\int_0^\infty R_A(\tau^* H)\cos 2\pi F\tau^* d\tau^* \tag{51}$$

where

$$R_A(\tau^* H) = E[A(x)A(x + \tau^* H)] = E\{A(HX)A[H(X + \tau^*)]\}$$
$$= E[A^*(X)A^*(X + \tau^*)] = R_{A^*}(\tau^*) \tag{52}$$

and

$$A(HX) = A^*(X) \tag{53}$$

where the operator denotes the expected value of the operand. Therefore, $S_A(\omega)$ can be written as

$$S_A(\omega) = HS_{A^*}(F) \tag{54}$$

Consider now the new frequency, $F = \omega H$. When $S_A(\omega)$ is known and the probability distribution of F is f_F, the theory of derived distributions can be used to write

$$f_F = \frac{1}{H} S_A\left(\frac{F}{H}\right) = \frac{1}{H} S_A(\omega) = S_{A^*}(F) \tag{55}$$

This result justifies equation 33, where the dimensionless frequencies F_k were distributed with a density function $S_{\ell n K^*}(F)\sigma^2_{\ell n K^*}$ (the division by $\sigma^2_{\ell n K^*}$ normalizes the frequency spectra function to obtain a unit area under the curve).